

A versatile Cas12k-based genetic engineering toolkit (C12KGET) for metabolic engineering in genetic manipulation-deprived strains

Yali Cui^{1,2,†}, Huina Dong^{1,2,†}, Baisong Tong^{1,2}, Huiying Wang^{1,2}, Xipeng Chen^{1,2}, Guangqing Liu^{1,2} and Dawei Zhang^{1,2,3,*}

¹Tianjin Institute of Industrial Biotechnology, Chinese Academy of Sciences, Tianjin 300308, China, ²National Technology Innovation Center of Synthetic Biology, Tianjin 300308, China and ³University of Chinese Academy of Sciences, Beijing 100049, China

Received January 26, 2022; Revised July 07, 2022; Editorial Decision July 08, 2022; Accepted July 22, 2022

ABSTRACT

The genetic modification of microorganisms is conducive to the selection of high-yield producers of high-value-added chemicals, but a lack of genetic tools hinders the industrialization of most wild species. Therefore, it is crucial to develop host-independent gene editing tools that can be used for genetic manipulation-deprived strains. The Tn7-like transposon from *Scytonema hofmanni* has been shown to mediate homologous recombination-independent genomic integration after heterologous expression in *Escherichia coli*, but the integration efficiency of heterologous sequences larger than 5 kb remains suboptimal. Here, we constructed a versatile Cas12k-based genetic engineering toolkit (C12KGET) that can achieve genomic integration of fragments up to 10 kb in size with up to 100% efficiency in challenging strains. Using C12KGET, we achieved the first example of highly efficient genome editing in *Sinorhizobium meliloti*, which successfully solved the problem that industrial strains are difficult to genetically modify, and increased vitamin B₁₂ production by 25%. In addition, Cas12k can be directly used for transcriptional regulation of genes with up to 92% efficiency due to its naturally inactivated nuclease domain. The C12KGET established in this study is a versatile and efficient marker-free tool for gene integration as well as transcriptional regulation that can be used for challenging strains with underdeveloped genetic toolkits.

INTRODUCTION

Microorganisms and their products are widely used in many fields, spanning the fine and bulk chemical industry, agriculture and medicine. Available tools can achieve specific modification at the genome level in model organisms, which is conducive to opening up the full potential of strains. Historically, these approaches have been limited to random gene insertions and mutations, or to limited modifications at pre-defined locations in the genome. The low homologous recombination ability also limits the genetic modification of strains. Notably, the integration of heterologous genes or biochemical pathways into the genome can avoid the metabolic burden of plasmid-based expression and precisely regulate metabolic fluxes (1–3), while also guaranteeing stable inheritance. The resulting engineered strains are more suitable for industrial applications, allowing long-term batch replenishment cultures without the need for expensive antibiotic selection. Therefore, the development of effective genomic integration techniques is of great importance for the rational modification of strains. Despite many recent advances in the programmable editing of bacterial and eukaryotic genomes, effective insertion of heterologous genes into specific loci remains a great challenge (4–8), and even simple random gene integration is not yet possible in some strains.

Sinorhizobium meliloti is a Gram-negative Alphaproteobacterium that is an intracellular nitrogen-fixing symbiont of legumes. Co²⁺ is an essential element for the growth of *S. meliloti* and is required for nitrogen fixation (9). Vitamin B₁₂, in a narrow sense, also known as cyanocobalamin, is a kind of cobalamin (Cbl) and the only vitamin containing the metal element, cobalt. The chemical structure of 5'-deoxyadenosylcobalamin consists of a central cobaltine ring (cobamide), an upper ligand (adenosine moiety) and a lower ligand (5,6-dimethylbenzimidazole, DMBI). The genome of *S. meliloti* contains a complete

*To whom correspondence should be addressed. Tel: +86 22 24828749; Email: zhang_dw@tib.cas.cn

†These authors contributed equally to this work.

set of genes encoding the aerobic Cbl biosynthesis pathway, which is capable of synthesizing Cbl *de novo* through an oxygen-dependent pathway (10). Cbl has been isolated from *S.meliloti* and was found to contain DMBI as a ligand (11). In addition, the Cbl-dependent enzymes methylmalonic acid coenzyme A mutase (CobA), methionine synthase and ribonucleotide reductase (12–14), as well as putative Cbl biosynthesis genes, were identified in *S.meliloti* (15). Therefore, *S.meliloti* can be used for industrial production of vitamin B₁₂, except for the feedback inhibition in its metabolic pathway. Moreover, the previous dominant strains were non-engineered, mainly due to their own low homologous recombination efficiency and lack of gene editing tools for genetic manipulation (16–18).

To date, researchers have developed gene integration tools that do not need to rely on native homologous recombination pathways in the target strain (19–22). During comparative genomics studies of clustered regularly interspaced palindromic repeats (CRISPR)/CRISPR-associated protein (CRISPR/Cas) systems, researchers identified the unique Type V CRISPR/Cas systems associated with transposon-specific genes (23), which led to the discovery of a Cas12k-based Tn7-like transposon (24). These Type V CRISPR/Cas systems encode effectors which are very similar to TnpB nucleases. These are considered a possible intermediate in the evolution of TnpB toward the classical type V CRISPR/Cas systems containing the Cas12 effector protein (25–27). However, the predicted effector protein Cas12k is smaller than the classical Cas9 and Cas12 proteins, contains a nuclease with a naturally inactivated RuvC-like nuclease domain and has no interference function (20). Cas12k and the adjacent CRISPR array are embedded in Tn7-like transposons that also contain characteristic terminal structures (LE and RE), with associated transposase genes *tnsB*, *tnsC* and *tniQ* (28). The system does not require the expression of fusion cassettes, and Cas12k is recruited to the target site by recognizing a protospacer adjacent motif (PAM), associated transposases and a cargo gene for unidirectional insertion of a donor sequence 60–66 bp downstream of the gene integration site (Figure 1A). Integration of ~10 kb DNA fragments into the *Escherichia coli* genome has been successfully achieved without positive selection, but the integration efficiency of fragments > 5 kb is still less than ideal (20).

In this study, we developed a versatile Cas12k-based genetic engineering toolkit (C12KGET) for genetic manipulation of challenging industrial strains, achieving 100% integration efficiency of heterologous DNA fragments up to 10 kb without the need for selection markers, as well as successfully down-regulating gene expression by 92%. Finally, we demonstrate that the tool can be used to rationally modify metabolic pathways, with the first successful modification of the genome of *S.meliloti*, which resulted in a 25% increase of vitamin B₁₂ production without affecting cell growth.

MATERIALS AND METHODS

Plasmid construction

The complete lists of all primers and single guide RNA (sgRNA) sequences used in this study are respectively pro-

vided in Supplementary Tables S1 and S2. All relevant integration plasmid constructs for *S.meliloti* were generated using a combination of Gibson assembly, restriction digestion and ligation. All polymerase chain reaction (PCR) fragments used for cloning were generated using Q5 DNA polymerase. Cloning reaction mixtures were directly used to transform NEB Turbo *E.coli*. Plasmids were extracted using Qiagen Miniprep columns and confirmed by Sanger sequencing (GENEWIZ). The pHelper plasmid (ID: 127921) and pDonor plasmid (ID: 127924) are available from Addgene.

The pDonor plasmid was used as a template to clone LE and RE into the pKP302 plasmid, resulting in pKP-1.5 k, pKP-2.5 k, pKP-5.5 k and pKP-10 k, according to the length of the cargo sequence, respectively. The corresponding transposase genes were cloned into the pKP302 plasmid from the pHelper plasmid, and all transposition assays in *S.meliloti* were performed by transformation with the CRISPR-associated transposase (CAST) expressed using the J23119 promoter. A series of pKP-target plasmids was constructed using Gibson assembly, named separately according to the targeting site. The pKP-Donor and pKP-target plasmids were used for transposition experiments in *S.meliloti*. Transformants were cultured in liquid TYC medium or on solid TYC agar plates with the addition of 600 mg/l spectinomycin for the pKP-Donor plasmid and 100 mg/l apramycin for the pKP-target plasmid.

The related CRISPR interference (CRISPRi) plasmid is mainly a pHelper plasmid as a template, with *cas12k* and sgRNA sequences loaded on the pKP plasmid, and the resistance gene is spectinomycin. Transformants were cultured in liquid TYC medium or on solid TYC agar plates with the addition of 600 mg/l spectinomycin for pKP-CRISPRi. For example, we constructed seven recombinant plasmids named pKP-Cas12k-gfp-5T, pKP-Cas12k-gfp-5NT, pKP-Cas12k-gfp-3T, pKP-Cas12k-gfp-3NT, pKP-Cas12k-gfp-ZT, pKP-Cas12k-gfp-ZNT and pKP-Cas12k-gfp-no, which were targeted to different sites of the *gfp* gene. The dCas9-associated plasmids were constructed according to the above process, and named pKP-dCas9-gfp-5T, pKP-dCas9-gfp-5NT, pKP-dCas9-gfp-3T, pKP-dCas9-gfp-3NT, pKP-dCas9-gfp-ZT, pKP-dCas9-gfp-ZNT and pKP-dCas9-gfp-no, which were targeted to different sites of the *gfp* gene. The sgRNA sequences are listed in Supplementary Table S2 and all plasmids are listed in Supplementary Table S3.

Sinorhizobium meliloti culture and general transposition assays

A complete list of *S.meliloti* strains used for transposition experiments is provided in Supplementary Table S4. All *S.meliloti* transposition experiments were performed with *S.meliloti* 320. The cells were cultured in TYC medium containing (1 l): 5 g of tryptone, 3 g of yeast extract and 0.67 g of CaCl₂. All *S.meliloti* transformations were performed using electrocompetent cells and standard electrotransformation methods, followed by recovery in TYC medium at 30°C and 200 rpm, and then selection on agar plates with the indicated antibiotics. The typical transformation efficiency was > 10³ colony-forming units/μg of total DNA.

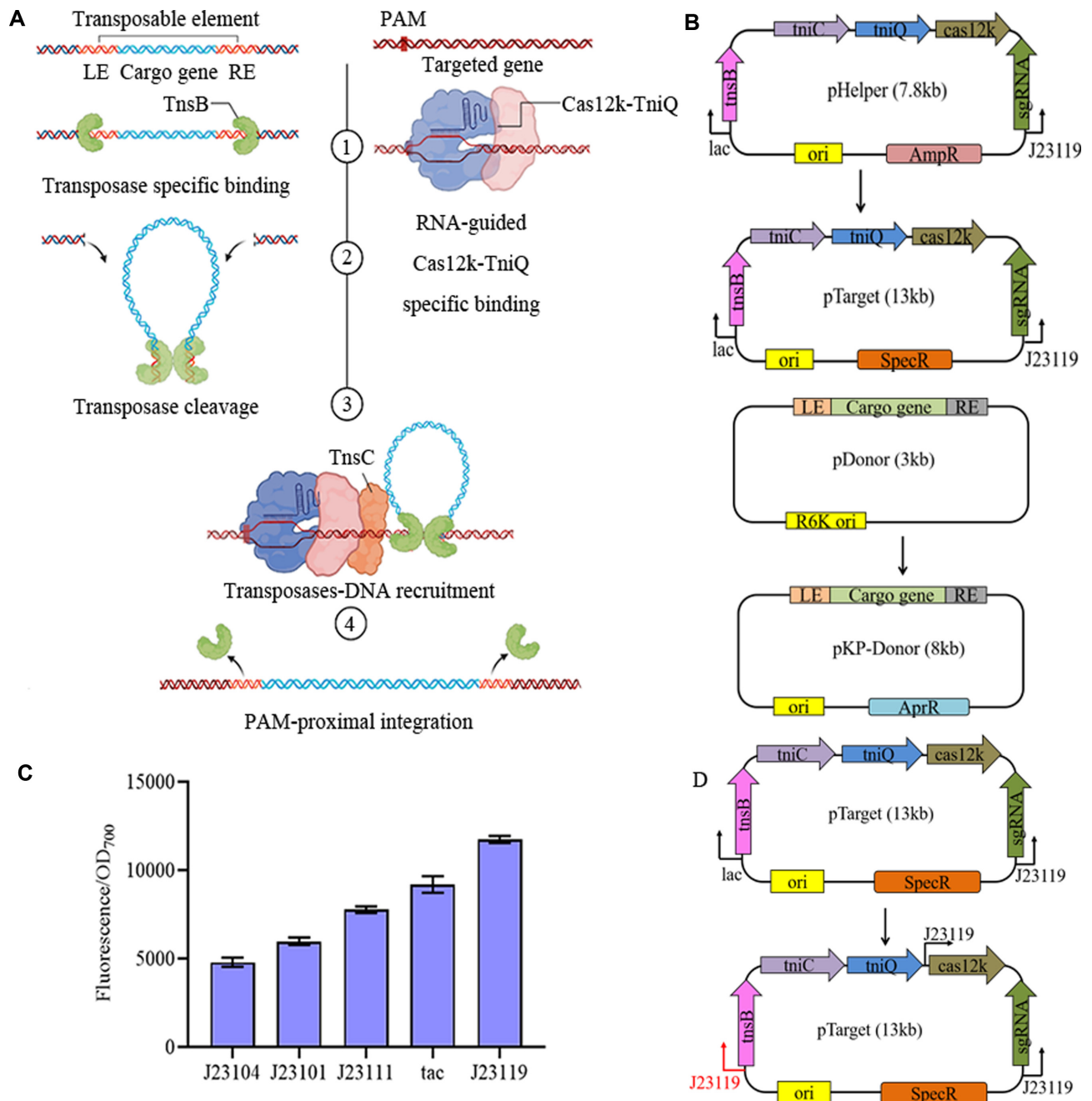


Figure 1. CAST can be used for gene integration in *S. meliloti*. **A.** Schematic of CAST-mediated gene integration. **B.** The pHelper and pDonor are schematic of the original CAST system, and the pTarget and pKP-Donor are the improved CAST based on the high-copy-number vector pKP that can replicate autonomously in *S. meliloti*. **C.** The fluorescence of the selected promoters. **D.** Constructed pTarget for *S. meliloti*. The original promoter in front of the transposase gene was replaced with the stronger J23119 promoter, which was also used to initiate the expression of Cas12k protein alone.

All standard transposition tests in *S. meliloti* included incubation at 30°C for 72 h after recovery and plate spreading.

Preparation of electrocompetent cells of *S. meliloti* and electrotransformation

Sinorhizobium meliloti 320 was streaked on TYC agar plates and incubated at 30°C for 3 days. A single colony was picked into 5 ml of TYC medium in a tube and incubated at 30°C for 24–28 h at 200 rpm. Then, the 5 ml bacterial culture

was transferred to a 250 ml flask containing 30 ml of TYC medium and incubated at 30°C for 5 h. When the OD₇₀₀ reached 0.6, the flask was placed in an ice bath for 30 min, transferred into a sterilized ice-cold 50 ml centrifuge tube and centrifuged at 4°C and 4000 rpm for 10 min. The supernatant was removed and the cells were resuspended in sterile ice-cold water and centrifuged as above. This step was repeated twice. Then, the cells were resuspended in ice-cold 10% glycerol and centrifuged as above. This step was also repeated twice. The cells were finally concentrated and

resuspended in 10 ml of ice-cold 10% glycerol, aliquoted and stored at -80°C . For transformation, 1 ml of electrocompetent cells was combined with 1 μg of donor DNA or plasmid, transferred into a 1 mm electroporation cuvette and electroschocked at 1.7 kV. The cells were cultured in TYC medium, placed in a 1.5 ml Eppendorf tube for recovery at 30°C and centrifuged at 200 rpm for 2 h. Then, the cells were spun down, spread on TYC agar plates with the indicated antibiotics, and grown at 30°C for 4–6 days until single colonies appeared.

Experiments involving the pKP-Donor and pKP-target were performed by first transforming electrocompetent cells with pKP-Donor, selecting individual colonies and growing them with antibiotic selection in TYC medium at 30°C for 3 days, and then pKP-target was transformed into the cells. Experiments involving the CRISPRi-targeted *gfp* gene necessitated transforming electrocompetent cells with pKP-Cas12k-*gfp* plasmids, and a clone containing the plasmid was incubated in resistance medium until $\text{OD}_{700} = 0.8$ and induced by adding 1 mM isopropyl- β -D-thiogalactopyranoside (IPTG). After 16 h induction, 50 μl of the bacterial solution was centrifuged to remove the supernatant, the slime was resuspended with 200 μl of ddH₂O and the fluorescence intensity was detected by a multifunctional enzyme marker. Experiments involving CRISPRi targeted to other endogenous genes necessitated transforming electrocompetent cells with pKP-Cas12k plasmids, and a clone containing the plasmid was incubated in resistance medium until $\text{OD}_{700} = 0.8$ and induced by adding 1 mM IPTG. After 16 h induction, the level of gene down-regulation was assessed by quantitative PCR (qPCR).

Transposition efficiency analysis by colony PCR and Sanger sequencing

Colony PCR was performed using *Taq* DNA polymerase and Green Taq Mix (Vazyme Biotech). A single clone was randomly picked from plates and suspended in 10 μl of H₂O as the DNA template for the PCR. The 20 μl reaction mixtures contained 10 μl of Green Taq Mix, 1 μM primer, 1 μl of template and 7 μl of H₂O. The thermal cycling conditions were: one cycle, 95°C , 5 min; 29 cycles, 95°C , 30 s, 55°C , 30 s, 72°C , 5 s; held at 4°C . Primer pairs were designed to be ~ 300 bp upstream of the insertion site and ~ 100 bp within the insertion gene near the LE in order to shorten the detection time. PCR products were separated by 1% agarose gels and stained with SYBR Safe (Thermo Scientific). Negative control samples and experimental samples were analyzed in parallel to identify non-specific bands. The PCR products were sent to GENEWIZ for isolation and analysis.

High-throughput sequencing and data analysis

The raw image data of sequencing results were identified by image base calling (Base calling) using the software CASAVA (v1.8.2), and preliminary quality analysis was performed to obtain the raw data of sequenced samples (Pass Filter Data, PF). The raw data were pre-processed and the low-quality data were filtered using Cutadapt software to remove primer contamination and spliced sequences. The

data were split according to the barcode sequences, and the target sequences were selected according to the up and downstream 10 nt of the target sequences, followed by calculation of the abundance statistics. The merged sequences were compared with the reference sequences using BWA software to extract statistical mutation abundance information, after which the frequencies of insertion at different sites were obtained.

Paired-end sequencing and off-target rate analysis

The genomic DNA of *S. meliloti* from a 5 ml culture with an OD_{700} of 2 was extracted using the Qiagen Genome Extraction Kit. Then, the DNA was fragmented, followed by end-complementation repair by adding a deoxynucleotide at the 3' end to convert to sticky ends. DNA connectors containing index sequences were then added on both sides of the sticky ends by complementary base pairing. PCR amplification was performed to add index sequences to the end of the target fragment to complete the construction of the sequencing library, which was bound to the sequencing chip by bridge PCR. The library was then sequenced by Illumina HiSeq onboard. The sequencing data were processed offline to obtain the raw data, which were filtered to remove connectors, decontaminated and then compared with the reference genome. From the results of the comparison, duplicate sequences due to PCR amplification were removed from each library, and then the sequencing depth and coverage relative to the reference genome were calculated. The insertion position was determined by finding chimeric sequences bridging the insert and the reference genome in the clean data.

Plasmid curing

The verified inserted clones were grown in 5 ml of TYC medium at 30°C and 200 rpm for 3 days. Then, 10 μl were transferred to 5 ml of TYC medium, cultured for 2 days; this was repeated six times. A 10 μl aliquot was streaked on TYC agar plates and grown at 30°C for 3 days. Single colonies were picked and replica-spotted on plates with no antibiotic, as well as plates with spectinomycin and plates with ampicillin, respectively. The clones that grew only on the antibiotic-free plates were selected as the cured strains.

Shaking flask studies

Shaking flask studies were performed in complex medium containing 50 g/l brown sugar, 60 g/l of corn syrup, 2 g/l $(\text{NH}_4)_2\text{SO}_4$, 0.006 g/l of CoCl_2 , 2.6 g/l KH_2PO_4 , 6 g/l betaine (*N,N,N*-trimethylglycine) and 1 g/l DMBI, pH 6.8–7.0. Seed cultures were grown in 5 ml of TYC medium at 30°C and 200 rpm for 20–24 h, until the OD_{700} reached 2–3. The cells were harvested in a 50 ml tube by centrifugation at 6000 rpm for 2 min, the supernatant was discarded and the cells were resuspended in 30 ml of TYC medium. Then, a 250 ml conical flask containing 30 ml of fermentation medium was inoculated at a ratio of 1:50 and sealed with an air-permeable aseptic film. The fermentations were conducted at 30°C and 200 rpm for 7 days.

Real-time PCR

The sample RNA was extracted by the TRIzol method, and the experimental operation was carried out according to the product instructions. The template RNA was thawed on ice, 1 µg was added to 2 µg of template RNA and 4 µl of 4× gDNA wiper Mix, and RNase-free H₂O was added to make up the volume to 16 µl; it was held at 42°C for 2 min. An additional 4 µl of 5× HiScript III qRT SuperMix was then added. The above reaction solution was incubated at 37°C for 15 min, then at 85°C for 5 s to terminate the reaction, and placed on ice for subsequent experiments or cryopreservation. PCR was carried out in a reaction system consisting of 5 µl of 2× Master Mix, 0.2 µl of Primer F, 0.2 µl of Primer R, 1 µl of cDNA and 3.6 µl of water. The target gene and internal reference of each sample were each subjected to real-time PCR (Applied Biosystems, QuantStudio™5), and each sample was tested in three replicate wells. The data were analyzed using the $2^{-\Delta\Delta CT}$ method (29) and the primers and PCR program are shown in Supplementary Table S7.

High-performance liquid chromatography (HPLC) analysis of the vitamin B₁₂ yield

The wells of a 96-well plate were filled with 870 µl of sterile water and 30 µl of bacterial culture, after which 200 µl of the resulting diluted suspension was moved to a microtiter plate to measure the OD₇₀₀. Samples comprising 1 ml of the fermentation broth were taken after 7 days of fermentation, and quenched by adding 100 µl of 8% sodium nitrite and 100 µl of glacial acetic acid. The quenched samples were centrifuged at 12 000 rpm for 2 min, the supernatant was removed, passed through a 0.22 µm pore-size membrane and combined with 20 µl of 2% NaCN (w/v). The analysis was conducted on an Agilent TC C18 column (4.6 × 250 mm) at a temperature of 35 °C. The mobile phase was prepared by vacuum filtration of water through a 0.22 µm pore-size aqueous membrane, followed by sonication for 30 min. The organic phase was methanol (HPLC grade), which was also sonicated for 30 min. The mobile phase consisted of 30% methanol and 70% water at a flow rate of 0.8 ml/min. The injection volume was 15 µl, the detection wavelength was 361 nm and the running time was 15 min.

RESULTS

Verification of CRISPR-associated transposase (CAST) system-mediated gene integration in *S.meliloti*

Sinorhizobium meliloti can be used for the industrial production of vitamin B₁₂, but its further optimization is hampered by a poor intrinsic homologous recombination ability and lack of effective gene editing tools. We transformed the fragment containing a 500 bp homology arm and a resistance gene, then randomly verified 10 single clones for verification. We found that no positive clones could be obtained through resistance screening. Subsequently, Cas9 protein was expressed through the tac promoter but clones could not be obtained (Supplementary Figure S1). However, modification of *S.meliloti* by means of genetic engineering enables the regulation of gene expression and modification of metabolic pathways to facilitate the selection of

high-yielding strains, so we urgently need to develop efficient gene editing tools in *S.meliloti*.

Cas12k-mediated CAST has been demonstrated to achieve the integration of DNA fragments with a size of up to 10 kb in *E.coli* with up to 80% efficiency using pHelper and pDonor plasmids (20). pHelper is a high-copy plasmid containing a colE1 replicon and encodes the transposase genes *tnsB*, *tnsC* and *tniQ*, as well as *cas12k* for targeting. pDonor contains the R6k replicon and is used to provide the cargo gene. To broaden the host range, we replaced the donor plasmid with the high-copy-number vector pKP, whose replication does not depend on the presence of the *pir* protein, which helps to improve the versatility of the resulting tool, named pKP-Donor. We integrated the transposase genes into a pKP plasmid with a different resistance marker, named pTarget (Figure 1B). After the pTarget targeting open reading frame (ORF) 1365 and the pKP-Donor loaded with a 2.5 kb cargo gene were electroporated into *S.meliloti*, 10 single clones were randomly selected to verify the efficiency of gene integration, and only five clones were found to have successful gene knock-ins (Supplementary Figure S2). Therefore, the tool still needed further optimization.

An optimized Cas12k-based gene integration tool in *S.meliloti*

Since previous experiments have shown that the efficiency of gene integration is directly proportional to the expression level of transposase (30), we screened a range of promoter strengths and characterized promoter strength by green fluorescent protein (GFP) (Figure 1C), and finally we selected the stronger J23119 promoter to improve the expression of transposase and Cas12k (Figure 1D). A total of 10 non-essential genes of *S.meliloti* (ORF 933, ORF 1354, ORF 1365, ORF 1699, ORF 1795, ORF 1797, ORF 1806, ORF 1807, ORF 1809 and ORF 4842) were selected as target sites, and the corresponding pTargets were constructed. The pKP-Donor-2.5kb vector with a cargo fragment length of 2.5 kb was selected as the donor plasmid. As shown in Figure 2A, we analyzed 10 randomly selected clones, all of which underwent integration. The strain which integrated the 2.5 kb cargo gene and targeted ORF 1365 was subjected to whole-genome sequencing to verify the off-target rate, and it was found that the main off-target site is in ORF 3194 (15.93%) (Supplementary Figure S3; Supplementary Table S6). Therefore, we concluded that the integration efficiency could be improved by adjusting the expression of the Tn7-like transposase and the tool could work in *S.meliloti* with high efficiency.

C12KGET-mediated efficient genome engineering in *S.meliloti*

To investigate the effect of different lengths of cargo fragments on editing efficiency, we selected ORF 933, ORF 1354 and ORF 1365 to integrate heterologous sequences of 1.5, 5.5 and 10 kb, respectively. As shown in Figure 1B and Supplementary Figure S4, the integration efficiency at all three sites was practically up to 100% without gene size limitation. After isolation of single clones and sequencing,

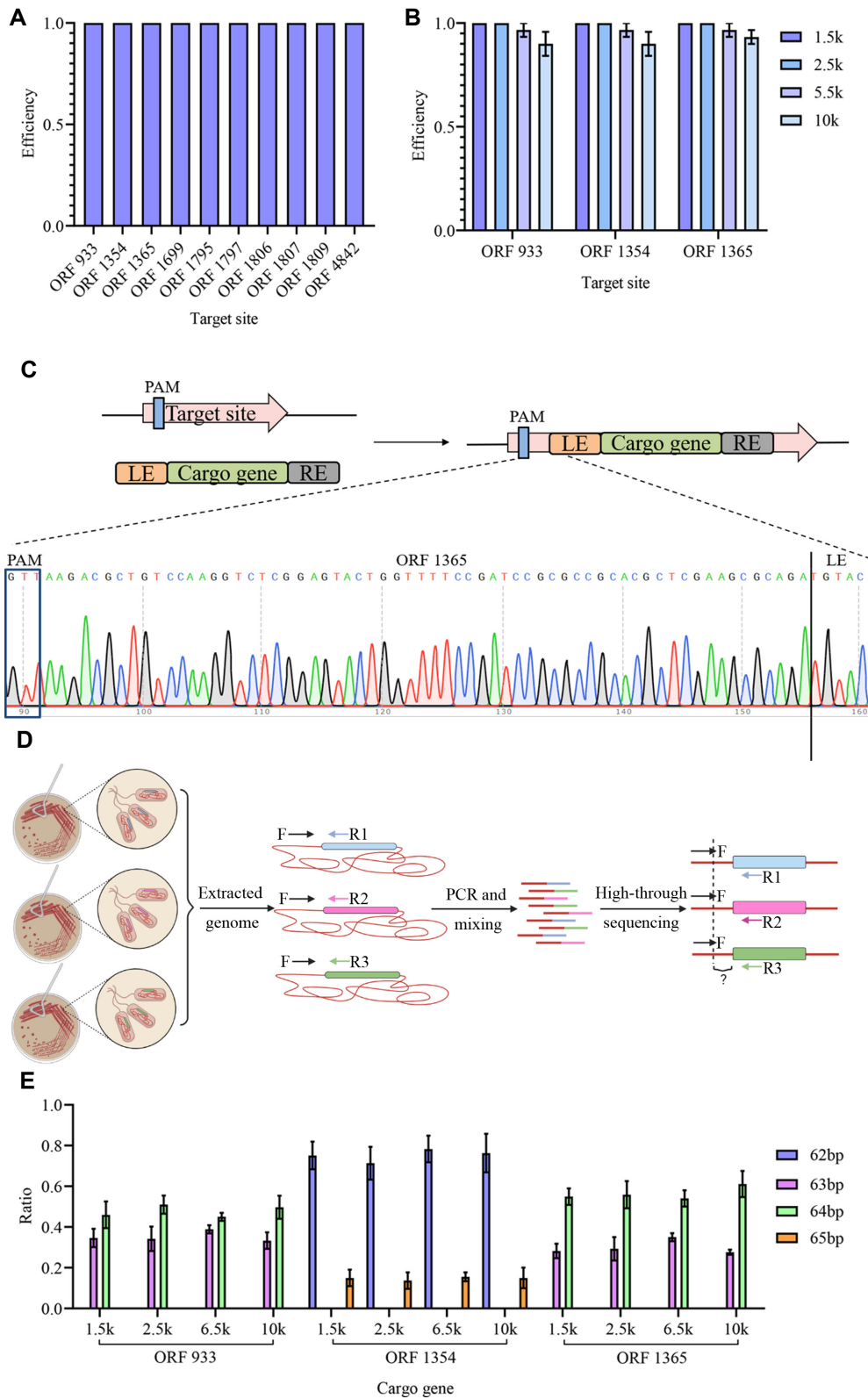


Figure 2. C12KGET enables high-efficiency insertion of large (10 kb) genetic payloads in *S. meliloti*. (A) PCR-based quantification of integration efficiency at different sites to insert a 2.5 kb gene. (B) PCR-based quantification of integration efficiency with different cargo sizes at three sites. (C) The sequencing result proves that the integration direction was at the left end of the transposon near the target site. (D) Schematic of high-throughput sequencing for insertion preference. (E) Integration sites have a preference as determined by high-throughput sequencing. Integration efficiency data in (A) and (B) are shown as the mean \pm SD for $n = 3$ biologically independent samples.

it was found that the integration direction was at the left end of the transposon near the target site, consistent with previous studies (Figure 2C; Supplementary Figure S5). These results showed that the constructed tool, C12KGET, could achieve efficient gene integration in *S.meliloti*, reaching practically 100% efficiency with cargo sequences of up to 10 kb.

Interestingly, when sequencing the above edited strains, we found a certain preference for the location of the insertion (Supplementary Figure S5). To explore the locus preference of gene integration, we took single clones with integrated donor sequences of 1.5, 2.5, 5.5 and 10 kb at ORF 933, ORF 1354 and ORF 1365 sites for culture, and extracted the genomic DNA for high-throughput sequencing (Figure 2D). Depending on the edited genes, gene integration at the same target site was stable despite the different lengths of the inserted donor sequences, mainly concentrated in two positions downstream of the PAM.

When integrating 1.5, 2.5, 5.5 and 10 kb donor sequences at ORF 933, gene integration occurred mainly at positions 63 and 64 bp downstream of the PAM, accounting for 40% and 35%, respectively. Gene integration at ORF 1354 occurred mainly at locations 62 and 65 bp downstream of the PAM, with proportions of 70% and 15%, respectively. Gene integration at ORF 1365 occurred mainly at 62 and 65 bp downstream of the PAM, with proportions of 55% and 30%, respectively (Figure 2E). Thus, the targeting position is rather fixed relative to the site downstream of the PAM, despite the different length of the donor fragment.

A novel Cas12k-based compact and strong transcriptional repression tool in *S.meliloti*

The Cas12k protein consists of only 639 amino acids and has a naturally inactivated endonuclease domain. By designing sgRNAs targeting the genome so that the Cas12k–sgRNA complex binds to the target gene, transcriptional elongation of the gene can be blocked and gene expression can be down-regulated. Compared with Cas9 and Cas12a, no mutation of the Cas protein is required, which gives it a natural advantage for transcriptional regulation.

To verify that Cas12k-mediated CRISPRi can down-regulate gene expression and the simplicity of the experimental operation, the *gfp* gene was selected as the target, and the down-regulation of expression was directly observed by measuring the change of GFP fluorescence. According to previous research results (31), targeting the same gene at different locations has different down-regulation effects. To allow a more comprehensive assessment of the effect of Cas12k-mediated CRISPRi, six different sites on the *gfp* gene were selected, three for each of the template and non-template strands (Figure 3A). Among them, plasmid pKP-Cas12k-gfp-no has no targeting site and was used as a negative control to characterize the interference-free fluorescence value. At the same time, we also constructed the corresponding dCas9-mediated transcriptional repression tool (Figure 3A) to verify the gene down-regulation effect of Cas12k-mediated CRISPRi.

The CY-1 strain (Supplementary Table S4) was constructed by integrating PJ23119-gfp into the genome using C12KGET, and was further used to verify whether Cas12k-

mediated CRISPRi can achieve transcriptional regulation in *S.meliloti*. The seven plasmids constructed above were individually introduced into the cells, and the fluorescence was detected in liquid cultures induced for 16 h. When the OD₇₀₀ reached 0.8, protein expression was induced by adding 1 mM IPTG. The experimental results showed that the effect differed greatly when targeting different positions of the target gene. Targeting 5' sequences of *gfp* on the chromosome resulted in the highest degree of down-regulation for both template and non-template strands (5T and 5NT), with up to 90% reduction of fluorescence. In contrast, the effect was poorer when targeting the 3' of *gfp*, which is consistent with dCas9-mediated transcriptional repression (Figure 3B).

We speculated that the best down-regulation effect can be achieved when targeting the 5' end of the template strand of the gene, and the worst down-regulation effect was achieved when targeting the 3' end of the non-template strand of the gene. The Cas protein–sgRNA complex binds to the 5'-untranslated region (UTR) of the DNA, preventing further mRNA extension by RNA polymerase, which in turn weakens the target gene expression. We also found that the effect of dCas9-mediated CRISPRi and Cas12k-mediated CRISPRi down-regulation of gene expression was consistent, but dCas9-mediated CRISPRi had a greater effect on bacterial growth (Figure 3C). Moreover, we also found that the fluorescence value decreased significantly after 6 h of induction (Figure 3D). In order to explore the effect of gRNA length on transcriptional regulation, we also truncated the gRNA, and tested the effect of 21 and 19 bp gRNA transcriptional regulation. At the same time, we also compared the effect of adding inducers at different times on transcriptional regulation. We found that the truncated gRNA could not effectively regulate the transcription of *gfp*, and the time of addition of inducers did not affect the effect of CRISPRi-mediated transcriptional regulation (Figure 3E). Thus, the high efficiency of Cas12k-mediated CRISPRi was also demonstrated in a genetic manipulation-deprived species.

C12KGET-mediated metabolic engineering in *S.meliloti*

Delta-aminolevulinic acid (ALA) is a common precursor for the synthesis of tetrapyrrole compounds such as vitamin B₁₂, heme and siroheme. In the C4 pathway, ALA is produced by the condensation of glycine with succinyl-CoA catalyzed by ALA synthase (HemA). Then, ALA molecules are assembled into porphobilinogen by ALA dehydratase (HemB), and further cyclized by bilirubinogen deaminase (HemC) and uroporphyrinogen III synthase (HemD) to form uroporphyrinogen III, which is the common precursor for the synthesis of heme, chlorophyll, siroheme and Cbl (Figure 4A). Since these tetrapyrrole compounds share the pathway from ALA to uroporphyrinogen III, enhancing their synthesis may also increase vitamin B₁₂ production. We used C12KGET to integrate the *hemA*, *hemB*, *hemC* and *hemD* genes (5.5 kb in total) into ORF 933 and ORF 1354, resulting in strains SM-1 and SM-2, respectively (Figure 4B). The qPCR data showed that the expression levels of *hemB*, *hemC* and *hemD* genes were up-regulated (Figure 4A). Since *hemA*, *hemB*, *hemC* and *hemD* are expressed

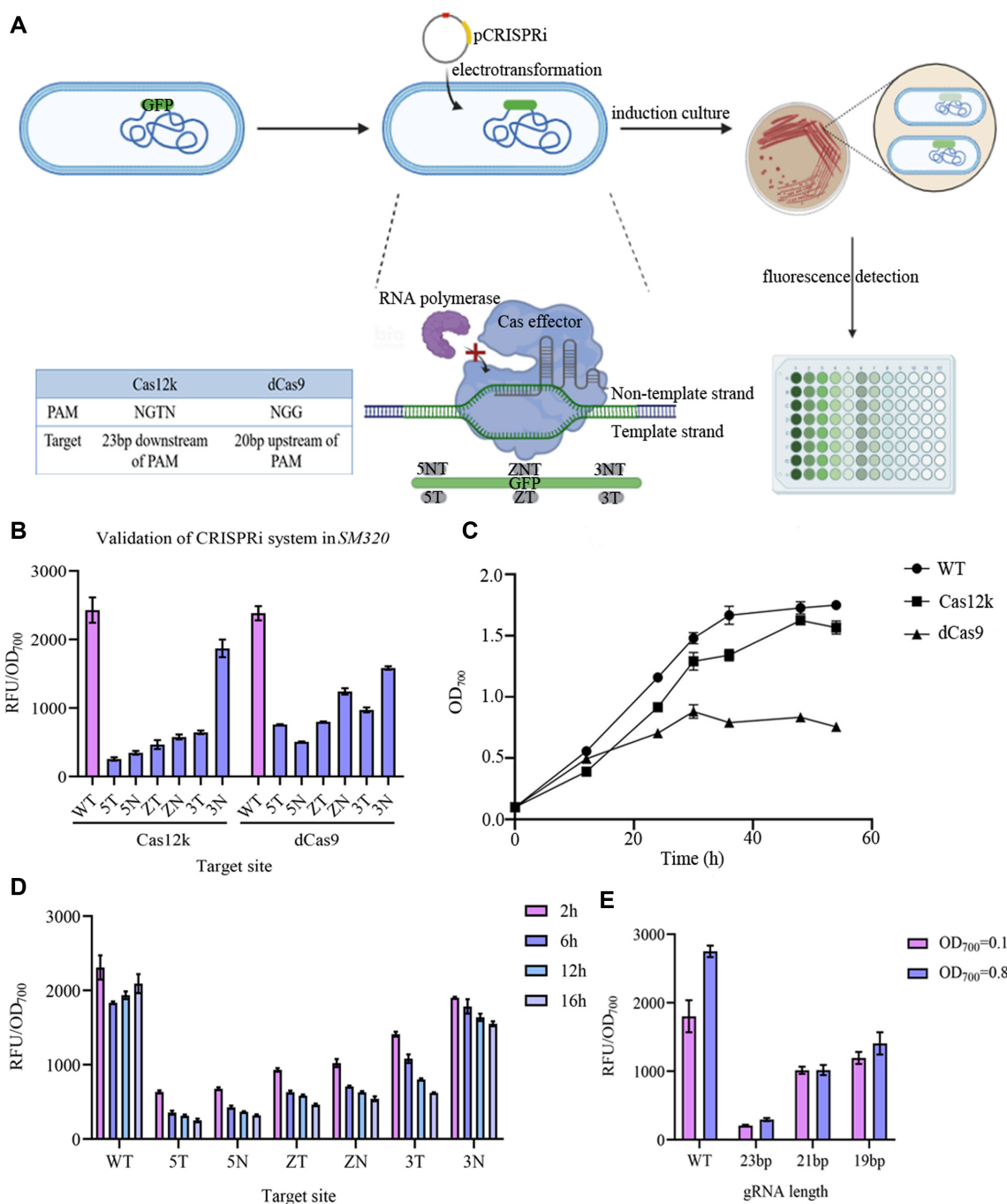


Figure 3. A novel CRISPRi tool based on Cas12k. (A) Schematic of Cas12k-mediated transcriptional regulation. (B) The effect of Cas12k- and dCas9-mediated CRISPRi in *S.melliloti*. (C) Growth curves of Cas12k- and dCas9-mediated CRISPRi in *S.melliloti*. (D) The effect of Cas12k-mediated CRISPRi in *S.melliloti* with different incubation times. (E). The effect of different sgRNA lengths and induction times on CRISPRi. Data in (B–E) are shown as the mean \pm SD for $n = 3$ biologically independent samples.

in fusion, it means that after the integration of the four genes, the expression of the genes has been up-regulated, and the engineered bacteria exhibited respective yield increases of $\sim 10\%$ and 15% (Figure 5B), while growth was unaffected compared with the wild type (Figure 4C). These results demonstrated that the promotion of ALA and uroporphyrinogen III synthesis can improve vitamin B₁₂ production.

Furthermore, feedback inhibition of enzymes located at nodes in the biosynthetic pathway is a common strategy for the regulation of microbial metabolism, and avoiding excessive synthesis of certain products can avoid wasting resources. In many bacteria, *S*-adenosyl-L-methionine:uroporphyrinogen III methyltransferase (SUMT) regulates the metabolic flow of Cbl. SUMT catalyzes the methylation of uroporphyrinogen III at po-

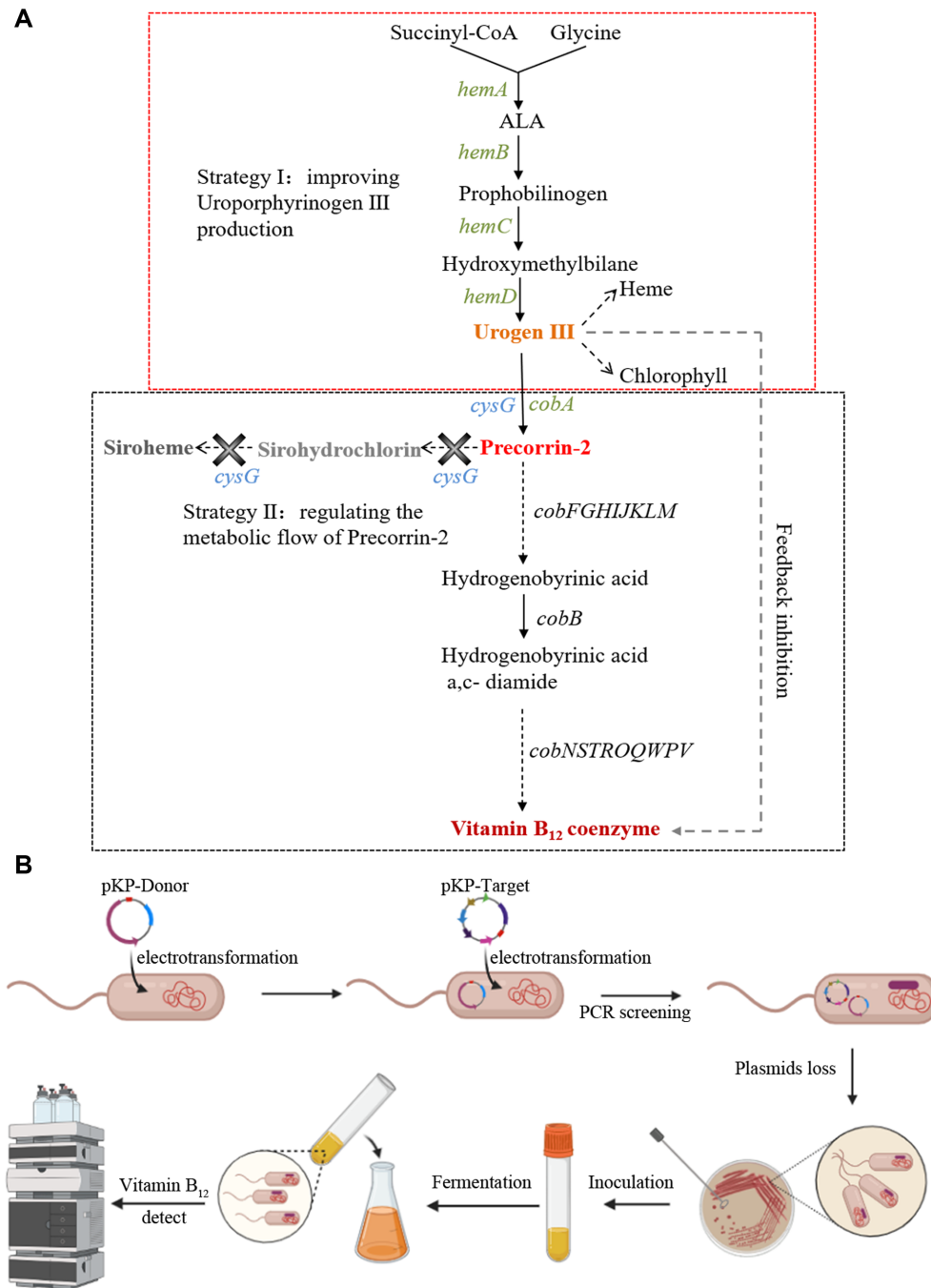


Figure 4. The biosynthetic pathway of vitamin B₁₂ in *S. meliloti* and different strategies to increase the production of vitamin B₁₂. **(A)** Schematic of the vitamin B₁₂ synthesis pathway of *S. meliloti*. At the uroporphyrinogen III node, the metabolic pathway is divided into two parts, and different regulatory strategies are adopted. The red box shows the uroporphyrinogen III synthesis module. The first strategy is to increase the production of uroporphyrinogen III by overexpressing *hemABCD* to provide sufficient substrate for the synthesis of vitamin B₁₂. The black box shows the siroheme by-product generation module. Strategy II aims to adjust the metabolic flow distribution of precirrin-2, reduce the generation of siroheme and avoid the consumption of precirrin-2 to promote the synthesis of vitamin B₁₂. **(B)** The process of strain construction, fermentation and vitamin B₁₂ detection in cultures of the engineered strains.

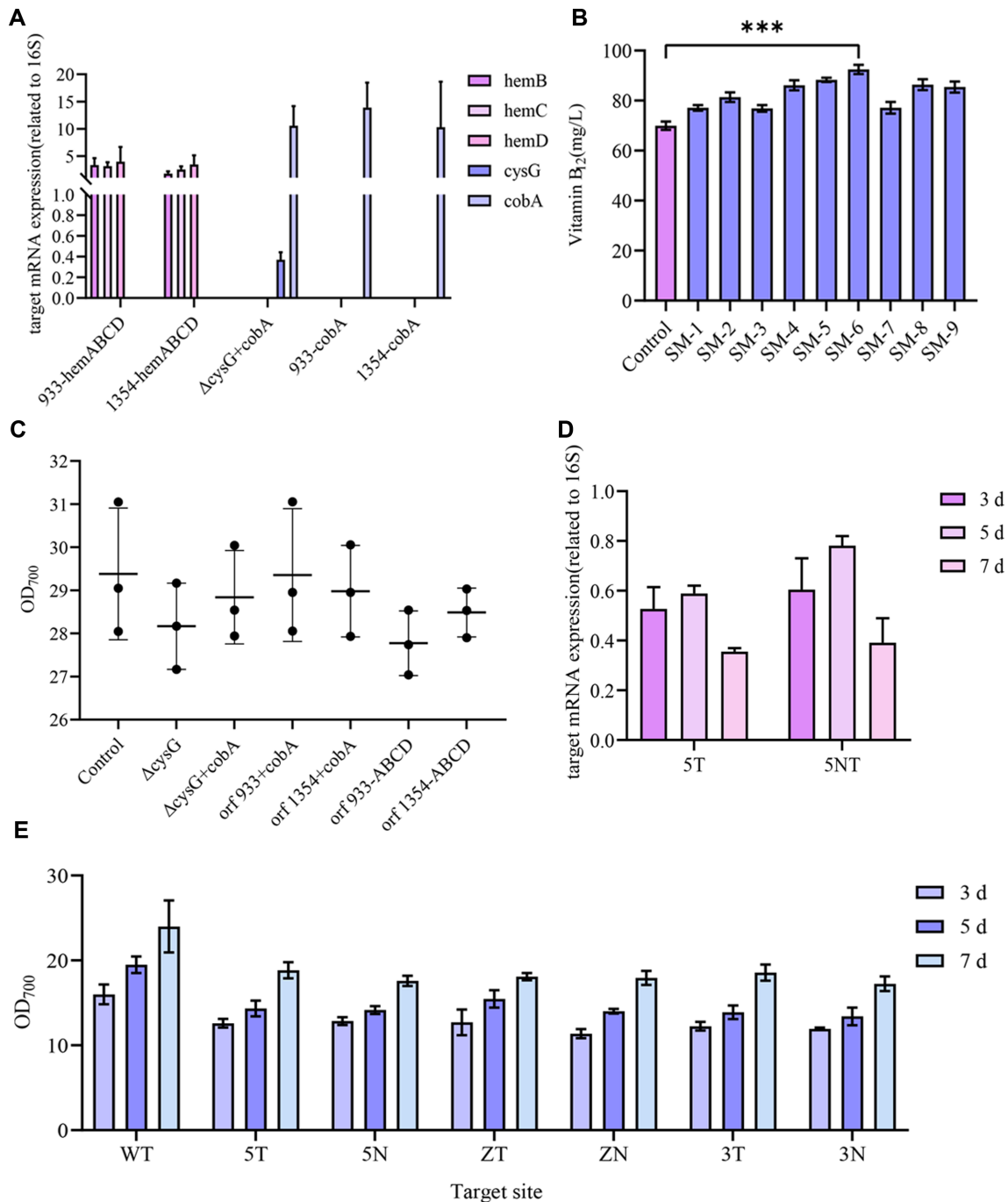


Figure 5. Transformation of *S. meliloti* using C12KGET successfully increased the yield of vitamin B₁₂. (A) The qPCR data of engineered strains overexpressing the *hemABCD* genes or *cobA* gene. (B) The vitamin B₁₂ production of engineered strains. (C) OD₇₀₀ of the six engineered strains after 7 days of fermentation without feeding. (D) The qPCR data of engineered strains with knockdown of the *cysG* gene. (E) OD₇₀₀ of the engineered strain constructed using CRISPRi to knock down the *cysG* gene after 2, 3 and 5 days of fermentation without feeding. Data in (A–E) are shown as the mean \pm SD for $n = 3$ biologically independent samples.

sitions 2 and 7 to generate precorrin-2, a key intermediate in the vitamin B₁₂ and siroheme biosynthesis pathways (Figure 4A) (32). It is subjected to feedback inhibition by an excess of the substrate uroporphyrinogen III and the product *S*-adenosyl-homocysteine (SAH) (33,34). Because of the presence of enzymatic substrate inhibition, feedback inhibition and multiple competing synthetic pathways, the

industrial yield of vitamin B₁₂ has remained stubbornly low, and it is necessary to optimize several common reactions in the synthesis of tetrapyrroles. CysG is a trifunctional enzyme that, together with CobA, catalyzes the conversion of uroporphyrinogen III to precorrin-2, which is further converted by a series of enzymes to produce vitamin B₁₂. Furthermore, the CysG enzyme converts precorrin-2 to

siroheme, one of the by-products of the vitamin B₁₂ biosynthesis pathway. Therefore, this metabolic pathway can be optimized either by targeting the *cysG* gene to reduce the production of siroheme from precorrin-2, thereby decreasing the consumption of precorrin-2, or alternatively by up-regulating the expression of *cobA* to avoid feedback inhibition due to uroporphyrinogen III overload, and promote the synthesis of precorrin-2 (Supplementary Table S5).

To reduce the production of siroheme, we down-regulated the expression of *cysG* using the CRISPRi tool. We took the fermentation broth at 3 and 5 days of fermentation, detected the expression of *cysG* at different fermentation times by qPCR and found that the gene expression was down-regulated during the fermentation process (Figure 5D). However, the fermentation of the constructed engineered strains revealed that the growth of the bacteria was affected by a large metabolic burden, slowing down by 40% compared with the wild type (Figure 5E). To avoid the metabolic burden caused by the plasmid and the toxicity caused by the inducer IPTG during fermentation, we chose to completely inactivate *cysG* by insertion of a transgene. When the integration site is selected in the ORF of the target gene, the inserted donor sequence causes a translational frameshift of the target gene, blocking its expression. The SM-3 strain was constructed by integrating the donor sequence into the ORF of the *cysG* gene.

In order to release the substrate repression of uroporphyrinogen III, the *cobA* gene was inserted into ORF 933 or ORF 1354, resulting in the strains SM-4 and SM-5, respectively. However, expressing only the *cobA* gene after blocking the *cysG* gene leads to insufficient precorrin-2 supply for vitamin B₁₂ synthesis. To avoid this, the *cobA* gene was integrated into the ORF of the *cysG* gene. The resulting strain SM-6 has no *cysG* gene expression while overexpressing the *cobA* gene. Previous studies have shown that *Rhodobacter capsulatus*-derived *cobA* (*RccobA*) can tolerate high substrate repression concentrations and can further unblock the substrate inhibition of SUMT (35). Therefore, we overexpressed *RccobA* in ORF 933 and ORF 1354, and integrated *RccobA* while blocking *cysG* to verify the effect on vitamin B₁₂ production, and named the strains SM-7, SM-8 and SM-9, respectively. The expression of the above genes was measured in the fermentation broth at the later stage of fermentation. qPCR data showed that the expression of all the above genes was up-regulated (Figure 5A). As shown in Figure 5B, the vitamin B₁₂ yields of the four gene-integrated strains increased compared with that of wild-type SM320, by ~10% in strain SM-3 and SM-7, and by 20% in strains SM-4, SM-5, SM-8 and SM-9. Notably, the vitamin B₁₂ yield of strain SM-6 was 92 mg/l, representing a 25% increase over the wild type. Importantly, growth was unaffected compared with the wild type (Figure 5C).

DISCUSSION

Currently, *S.meliloti*, the strain primarily used for vitamin B₁₂ production, can synthesize vitamin B₁₂ under aerobic conditions (36). The vitamin B₁₂ biosynthesis pathway involves > 30 genes (37), but several genes and regulatory feedback mechanisms have not been fully identified,

which makes the optimization of vitamin B₁₂ production extremely difficult (38,39). Due to the fact that homologous recombination efficiency of *S.meliloti* is low and is devoid of genetic manipulation tools, obtaining high-performance strains is mainly based on random mutagenesis (10). Previous experiments demonstrated that Ptac expression of Cas9 could not produce transformants, and we suspected that this may be due to the high expression of Cas9 protein, so it was further optimized by reducing the expression of Cas9. We found that a small number of transformants could be obtained by replacing the tac promoter with the lac promoter. Subsequently, the pKP plasmid contained the *cas9* gene and homology arm (500 bp) to make the 2.5 kb fragment integrate into ORF 933, ORF 1354 and ORF 1365, and even random selection of 20 clones can result in no positive clones, making genetic modification of this strain very challenging (Supplementary Figure S6).

In this study, we developed C12KGET, which resulted in genome modification of *S.meliloti* with an editing efficiency approaching 100% for the first time, and the integration efficiency of fragments >5 kb was significantly improved by increasing the expression of transposase. To simplify the procedure, we tried to integrate the dual-plasmid system into a single plasmid system (Supplementary Figure S7), but failed to achieve 2.5 kb gene integration at ORF 933, ORF 1354 or ORF 1365. In order to further explore the limit of the integration ability of this tool, we further tried to integrate an 11 kb cargo gene at ORF 1365. Unfortunately, although we randomly verified 10 single clones, no positive clones were obtained (Supplementary Figure S8).

The vitamin B₁₂ synthesis pathway is subject to feedback inhibition by various regulatory mechanisms, resulting in a strong repressive effect when vitamin B₁₂ accumulates in the cells, which may affect the expression of genes associated with vitamin B₁₂ synthesis (40). Uroporphyrinogen III is a common precursor for the synthesis of heme, chlorophyll, siroheme and vitamin B₁₂ (41). Therefore, we adopted a strategy of overexpressing *cobA* while inactivating *cysG*. Using this dual-plasmid technique, we successfully modified the vitamin B₁₂ synthesis pathway to increase the yield of vitamin B₁₂ by 25%, with no supplementation during fermentation.

In addition, to investigate the metabolic pathway of vitamin B₁₂, we integrated *cobI* (SM-11, SM-12), *cobF*, *cobG*, *cobH*, *cobI*, *cobJ*, *cobK*, *cobL* and *cobM* (SM-13, SM-14) and *cobN*, *cobS*, *cobT*, *cobO*, *cobQ*, *cobW* and *cobP* (SM-15, SM-16) in both ORF 933 and ORF 1354. It was found that the yield of vitamin B₁₂ increased by 15% for SM-11 and SM-12, 19% for SM-13 and SM-14, and 10% for SM-15 and SM-16 after 7 days of non-supplemented fermentation compared with the wild type. Since simultaneous expression of multiple genes by one J23119 promoter may result in insufficient expression of some genes, subsequent integration of single genes followed by integration of multiple genes for overexpression can be performed to further resolve the rate-limiting enzymes of the vitamin B₁₂ metabolic pathway and thus increase the yield of vitamin B₁₂ (Supplementary Figure S9). This technique greatly facilitates the modification of industrial strains lacking a native genetic engineering toolbox, and it is currently the first efficient genome editing tool available for *S.meliloti*.

Moreover, we also successfully achieved efficient gene integration in *Shewanella* sp. S05 (Supplementary Figure S10), which has low homologous recombination efficiency and lacks genetic editing tools (42). This strain also plays a crucial role in aquatic spoilage, and the method can be used to explore the mechanism of such spoilage of aquatic products (43). This demonstrates that C12KGET is a powerful tool for genetic modification of strains with low homologous recombination efficiency. Therefore, this tool will greatly simplify the metabolic engineering of a broad spectrum of industrial strains and will aid in studying the mechanisms of regulation of spoilage in aquatic products.

Despite these encouraging results, there are still many problems in this system that need to be further optimized. We sequenced the whole genome and found that the off-target rate was 17.48% in the whole ORF for sgRNA-3 (Supplementary Figure S3), and the major off-target sites are located within ORF 3194 where the integrated genes are located (15.93%). Since C12KGET in *S. meliloti* resulted in a low off-target rate within the ORF, this tool allows for precise gene integration to regulate metabolic pathways. Enhancing the ability of Cas protein to bind DNA or shortening the time of Cas protein searching for PAM may be one of the strategies to reduce its off-target rate, which makes C12KGET a convenient and widely applicable genetic tool.

Because there is no TnsA protein, this tool led to co-integration. According to Zhang *et al.*, the ratio of co-integration and simple integration in *E. coli* is 1:4 and, by pre-treatment of pDonor plasmid, single-strand nicks can effectively avoid the occurrence of co-integration (44). In addition, according to Tou *et al.*, a homing endonuclease and TnsB fusion and modified donor plasmid will be used to achieve a HELIX that can design and efficiently cut and ligate DNA insertions similar to type I CRISPR-related transposase technology that realizes programmable, unidirectional, independent recombination of DNA insertion technology and purifies simple insertion gene products with the smallest components and the smallest sized equipment, and the proportion of simple integration is as high as 99.3% (45).

In conclusion, C12KGET is compact, simple in composition and efficiently realizes gene editing and integration of large fragments of DNA unidirectionally, which can be used as a favorable tool for genetic manipulation-deprived strains to produce blocked gene expression, gene integration and transcriptional regulation by a single transformation. Especially for industrial strains such as *S. meliloti*, which can produce high-value chemicals, C12KGET lays the foundation for further yield improvement. We have used this tool to initially modify the vitamin B₁₂ pathway to obtain a high-yielding strain, which also indicates the potential for further development of this strain's ability to produce vitamin B₁₂.

DATA AVAILABILITY

High-through sequencing data are available in the NCBI Sequence Read Archive (BioProject accession code PRJNA798570). Published genomes used for analyses were obtained from the NCBI (RefSeq NC.000913.3). Datasets generated and analyzed in the current study, as well as cus-

tom scripts used for the described data analyses, are available from the corresponding author upon reasonable request.

SUPPLEMENTARY DATA

Supplementary Data are available at NAR Online.

FUNDING

The National Key R&D Program of China (grant/award no. 2018YFD0901001); National Natural Science Foundation of China (grant/award no. 22178372); Tianjin Synthetic Biotechnology Innovation Capacity Improvement Project (grant/award no. TSBICIP-CXRC-046, TSBICIP-CXRC-055 and TSBICIP-KJGG-011). Funding for open access charge: National Key R&D Program of China, National Natural Science Foundation of China and Tianjin Synthetic Biotechnology Innovation Capacity Improvement Project.

Conflict of interest statement. None declared.

REFERENCES

- Da Silva, N.A. and Srikrishnan, S. (2012) Introduction and expression of genes for metabolic engineering applications in *Saccharomyces cerevisiae*. *FEMS Yeast Res.*, **12**, 197–214.
- Zhang, Z., Moo-Young, M. and Chisti, Y. (1996) Plasmid stability in recombinant *Saccharomyces cerevisiae*. *Biotechnol. Adv.*, **14**, 401–435.
- Carrier, T., Jones, K.L. and Keasling, J.D. (1998) mRNA stability and plasmid copy number effects on gene expression from an inducible promoter system. *Biotechnol. Bioeng.*, **59**, 666–672.
- Pawelczak, K.S., Gavande, N.S., VanderVere-Carozza, P.S. and Turchi, J.J. (2018) Modulating DNA repair pathways to improve precision genome engineering. *ACS Chem. Biol.*, **13**, 389–396.
- Wang, H.H., Isaacs, F.J., Carr, P.A., Sun, Z.Z., Xu, G., Forest, C.R. and Church, G.M. (2009) Programming cells by multiplex genome engineering and accelerated evolution. *Nature*, **460**, 894–898.
- Vento, J.M., Crook, N. and Beisel, C.L. (2019) Barriers to genome editing with CRISPR in bacteria. *J. Ind. Microbiol. Biotechnol.*, **46**, 1327–1341.
- Perutka, J., Wang, W., Goerlitz, D. and Lambowitz, A.M. (2004) Use of computer-designed group II introns to disrupt *Escherichia coli* DEXH/D-box protein and DNA helicase genes. *J. Mol. Biol.*, **336**, 421–439.
- St-Pierre, F., Cui, L., Priest, D.G., Endy, D., Dodd, I.B. and Shearwin, K.E. (2013) One-step cloning and chromosomal integration of DNA. *ACS Synth. Biol.*, **2**, 537–541.
- Delwiche, C.C., Johnson, C.M. and Reisenauer, H.M. (1961) Influence of cobalt on nitrogen fixation by *Medicago*. *Plant Physiol.*, **36**, 73–78.
- Dong, H., Li, S., Fang, H., Xia, M., Zheng, P., Zhang, D. and Sun, J. (2016) A newly isolated and identified vitamin B12 producing strain: *Sinorhizobium meliloti* 320. *Bioprocess Biosyst Eng.*, **39**, 1527–1537.
- Kliewer, M. and Evans, H.J. (1962) Effect of cobalt deficiency on the B12 coenzyme content of *Rhizobium meliloti*. *Arch. Biochem. Biophys.*, **97**, 427–429.
- Cowles, J.R., Evans, H.J. and Russell, S.A. (1969) B12 coenzyme-dependent ribonucleotide reductase in rhizobium species and the effects of cobalt deficiency on the activity of the enzyme. *J. Bacteriol.*, **97**, 1460–1465.
- Cowles, J.R. and Evans, H.J. (1968) Some properties of the ribonucleotide reductase from *Rhizobium meliloti*. *Arch. Biochem. Biophys.*, **127**, 770–778.
- Sato, K., Inukai, S. and Shimizu, S. (1974) Vitamin B12-dependent methionine synthesis in *Rhizobium meliloti*. *Biochem. Biophys. Res. Commun.*, **60**, 723–728.
- Becker, A., Barnett, M.J., Capela, D., Dondrup, M., Kamp, P.B., Krol, E., Linke, B., Rüberg, S., Runte, K., Schroeder, B.K. *et al.* (2009) A portal for rhizobial genomes: RhizoGATE integrates a

- Sinorhizobium meliloti* genome annotation update with postgenome data. *J. Biotechnol.*, **140**, 45–50.
16. Liu, X., Li, P., Wang, Y. and Xie, Z. (2015) Deletion mutagenesis of Sma0955 genes in *Sinorhizobium meliloti* effect alfalfa growth. *J. Invest. Med.*, **63**, S51.
 17. Pieńko, T. and Trylska, J. (2017) Transport of vitamin B12 and its conjugate with peptide nucleic acid through the *E. coli* BtuB outer membrane protein explored with steered molecular dynamics. *Biophys. J.*, **112**, 504a.
 18. Luzader, D.H., Clark, D.E., Gonyar, L.A. and Kendall, M.M. (2013) EutR is a direct regulator of genes that contribute to metabolism and virulence in enterohemorrhagic *Escherichia coli* O157:H7. *J. Bacteriol.*, **195**, 4947–4953.
 19. Klompe, S.E., Vo, P.L.H., Halpin-Healy, T.S. and Sternberg, S.H. (2019) Transposon-encoded CRISPR-Cas systems direct RNA-guided DNA integration. *Nature*, **571**, 219–225.
 20. Strecker, J., Ladha, A., Gardner, Z., Schmid-Burgk, J.L., Makarova, K.S., Koonin, E.V. and Zhang, F. (2019) RNA-guided DNA insertion with CRISPR-associated transposases. *Science*, **365**, 48–53.
 21. Vo, P.L.H., Ronda, C., Klompe, S.E., Chen, E.E., Acree, C., Wang, H.H. and Sternberg, S.H. (2021) CRISPR RNA-guided integrases for high-efficiency, multiplexed bacterial genome engineering. *Nat. Biotechnol.*, **39**, 480–489.
 22. Yang, S., Zhang, Y., Xu, J., Zhang, J., Zhang, J., Yang, J., Jiang, Y. and Yang, S. (2021) Orthogonal CRISPR-associated transposases for parallel and multiplexed chromosomal integration. *Nucleic Acids Res.*, **49**, 10192–10202.
 23. Makarova, K.S., Wolf, Y.I., Alkhnbashi, O.S., Costa, F., Shah, S.A., Saunders, S.J., Barrangou, R., Brouns, S.J., Charpentier, E., Haft, D.H. et al. (2015) An updated evolutionary classification of CRISPR-Cas systems. *Nat. Rev. Microbiol.*, **13**, 722–736.
 24. Peters, J.E., Makarova, K.S., Shmakov, S. and Koonin, E.V. (2017) Recruitment of CRISPR-Cas systems by Tn7-like transposons. *Proc. Natl Acad. Sci. USA*, **114**, E7358–E7366.
 25. Faure, G., Shmakov, S.A., Yan, W.X., Cheng, D.R., Scott, D.A., Peters, J.E., Makarova, K.S. and Koonin, E.V. (2019) CRISPR-Cas in mobile genetic elements: counter-defence and beyond. *Nat. Rev. Microbiol.*, **17**, 513–525.
 26. Shmakov, S., Smargon, A., Scott, D., Cox, D., Pyzocha, N., Yan, W., Abudayyeh, O.O., Gootenberg, J.S., Makarova, K.S., Wolf, Y.I. et al. (2017) Diversity and evolution of class 2 CRISPR-Cas systems. *Nat. Rev. Microbiol.*, **15**, 169–182.
 27. Koonin, E.V. and Makarova, K.S. (2017) Mobile genetic elements and evolution of CRISPR-Cas systems: all the way there and back. *Genome Biol. Evol.*, **9**, 2812–2825.
 28. Querques, I., Schmitz, M., Oberli, S., Chanez, C. and Jinek, M. (2021) Target site selection and remodelling by type v CRISPR-transposon systems. *Nature*, **599**, 497–502.
 29. Pfaffl, M.W. (2001) A new mathematical model for relative quantification in real-time RT-PCR. *Nucleic Acids Res.*, **29**, e45.
 30. Vo, P.L.H., Ronda, C., Klompe, S.E., Chen, E.E., Acree, C., Wang, H.H. and Sternberg, S.H. (2021) CRISPR RNA-guided integrases for high-efficiency, multiplexed bacterial genome engineering. *Nat. Biotechnol.*, **39**, 480–489.
 31. Qi, L.S., Larson, M.H., Gilbert, L.A., Doudna, J.A., Weissman, J.S., Arkin, A.P. and Lim, W.A. (2013) Repurposing CRISPR as an RNA-guided platform for sequence-specific control of gene expression. *Cell*, **152**, 1173–1183.
 32. Sattler, I., Roessner, C.A., Stolorowich, N.J., Hardin, S.H., Harris-Haller, L.W., Yokubaitis, N.T., Murooka, Y., Hashimoto, Y. and Scott, A.I. (1995) Cloning, sequencing, and expression of the uroporphyrinogen III methyltransferase cobA gene of *Propionibacterium freudenreichii* (shermanii). *J. Bacteriol.*, **177**, 1564–1569.
 33. Robin, C., Blanche, F., Cauchois, L., Cameron, B., Couder, M. and Crouzet, J. (1991) Primary structure, expression in *Escherichia coli*, and properties of S-adenosyl-L-methionine:uroporphyrinogen III methyltransferase from *Bacillus megaterium*. *Am. Soc. Microbiol.*, **173**, 4893–4896.
 34. Storbeck, S., Walther, J., Müller, J., Parmar, V., Schiebel, H.M., Kemken, D., Dülcks, T., Warren, M.J. and Layer, G. (2009) The *Pseudomonas aeruginosa* nirE gene encodes the S-adenosyl-L-methionine-dependent uroporphyrinogen III methyltransferase required for heme d(1) biosynthesis. *FEBS J.*, **276**, 5973–5982.
 35. Storbeck, S., Walther, J., Müller, J., Parmar, V., Schiebel, H.M., Kemken, D., Dülcks, T., Warren, M.J. and Layer, G. (2009) The *Pseudomonas aeruginosa* nirE gene encodes the S-adenosyl-L-methionine-dependent uroporphyrinogen III methyltransferase required for heme d(1) biosynthesis. *FEBS J.*, **276**, 5973–5982.
 36. Taga, M. and Walker, G. (2010) *Sinorhizobium meliloti* requires a cobalamin-dependent ribonucleotide reductase for symbiosis with its plant host. *Mol. Plant Microbe Interact.*, **23**, 1643–1654.
 37. Guo, M. and Chen, Y. (2018) Coenzyme cobalamin: biosynthesis, overproduction and its application in dehalogenation—a review. *Rev. Environ. Sci. Bio/Technol.*, **17**, 259–284.
 38. Calderon-Ospina, C.-A. and Nava-Mesa, M. (2019) B vitamins in the nervous system: current knowledge of the biochemical modes of action and synergies of thiamine, pyridoxine, and cobalamin. *CNS Neurosci. Ther.*, **26**, 5–13.
 39. Bernhardt, C., Zhu, X., Schütz, D., Fischer, M. and Bisping, B. (2019) Cobalamin is produced by *Acetobacter pasteurianus* DSM 3509. *Appl. Microbiol. Biotechnol.*, **103**, 3875–3885.
 40. Polaski, J., Holmstrom, E., Nesbitt, D. and Batey, R. (2016) Mechanistic insights into cofactor-dependent coupling of RNA folding and mRNA transcription/translation by a cobalamin riboswitch. *Cell Rep.*, **15**, 1100–1110.
 41. Roessner, C.A., Huang, K.X., Warren, M.J., Raux, E. and Scott, A.I. (2002) Isolation and characterization of 14 additional genes specifying the anaerobic biosynthesis of cobalamin (vitamin B12) in propionibacterium freudenreichii (*P. shermanii*). *Microbiology (Reading)*, **148**, 1845–1853.
 42. Courts, A.D., Thomason, L.C., Gill, R.T. and Gralnick, J.A. (2019) Efficient and precise genome editing in *Shewanella* with recombineering and CRISPR-Cas9-mediated counter-selection. *ACS Synth Biol*, **8**, 1877–1889.
 43. Zhou, H., Gai, Y.M., Xu, C., Fu, S.P., Lin, X.P. and Zhang, D.W. (2021) Based on 16 s rDNA sequencing and culture medium method to explore the dominant spoilage bacteria in storage of rainbow trout. *J. Microbiol.*, **41**, 25–32.
 44. Strecker, J., Ladha, A., Gardner, Z., Schmid-Burgk, J.L., Makarova, K.S., Koonin, E.V. and Zhang, F. (2020) Response to comment on “RNA-guided DNA insertion with CRISPR-associated transposases”. *Science*, **368**, eabb2920.
 45. Tou, C.J., Orr, B. and Kleinstiver, B.P. (2022) Cut-and-Paste DNA insertion with engineered type V-K CRISPR-associated transposases. bioRxiv doi: <https://doi.org/10.1101/2022.01.07.475005>, 09 January 2022, preprint: not peer reviewed.